Supplementary Materials for

Structural basis of ER-associated protein degradation mediated by the Hrd1 ubiquitin ligase complex

Xudong Wu[1], Marc Siggel[2], Sergey Ovchinnikov[3], Wei Mi[4,5], Vladimir Svetlov[6], Evgeny Nudler[6], Maofu Liao[5], Gerhard Hummer[2,7], and Tom A. Rapoport1[$]

Correspondence to: tom_rapoport@hms.harvard.edu

This PDF file includes:

Figs. S1 to S18
Tables S1 ; S2

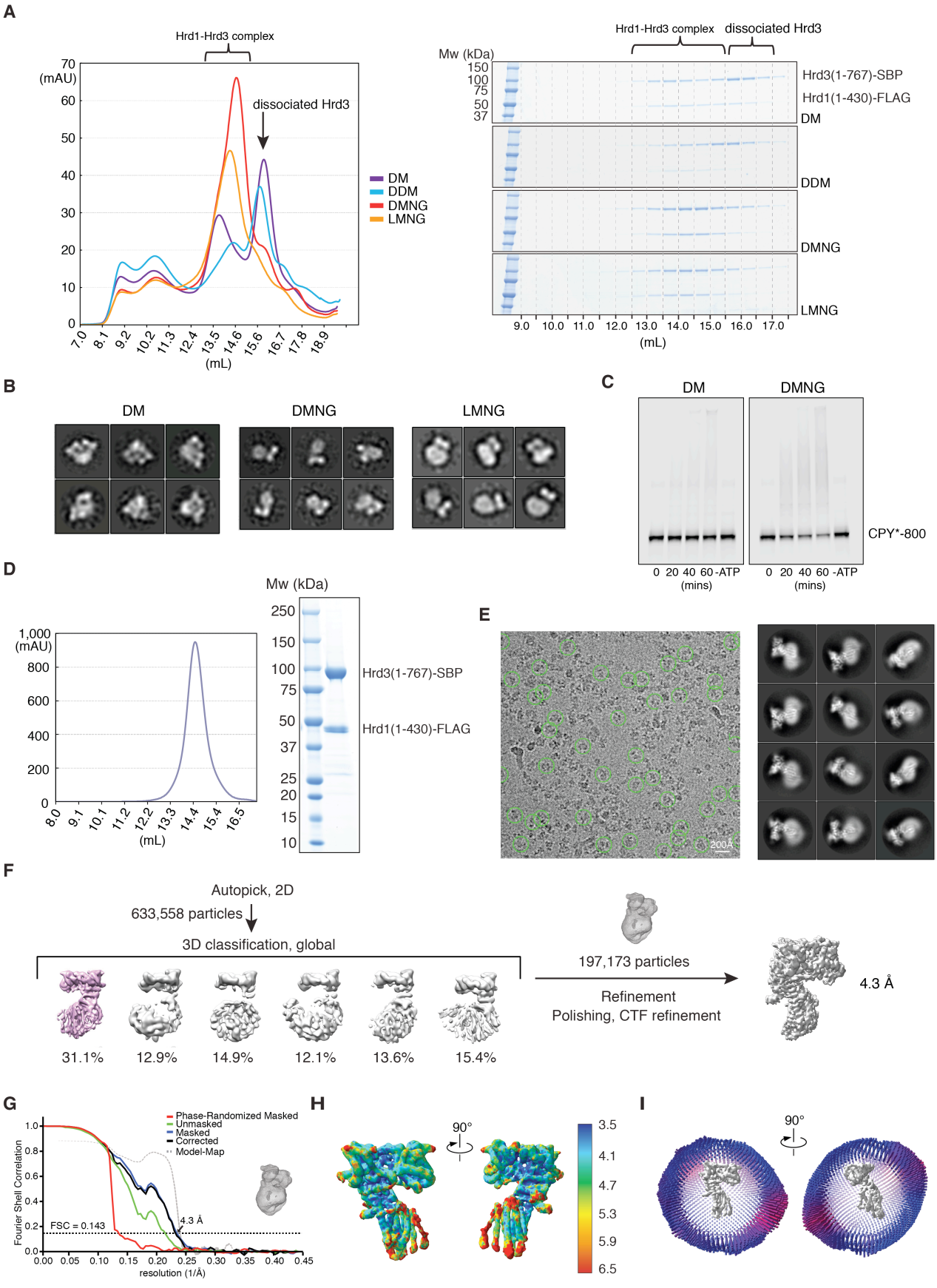
A
Hrd1-Hrd3 complex
dissociated Hrd3
(mAU)
(mL)
DM
DDM
DMNG
LMNG
Mw (kDa)
Hrd3(1-767)-SBP
Hrd1(1-430)-FLAG
B
C
CPY*-800
-ATP
(mins)
D
E
200Å
F
Autopick, 2D
633,558 particles
3D classification, global
31.1%
12.9%
14.9%
12.1%
13.6%
15.4%
197,173 particles
Refinement
Polishing, CTF refinement
4.3 Å
G
Phase-Randomized Masked
Unmasked
Masked
Corrected
Model-Map
Fourier Shell Correlation
FSC = 0.143
resolution (1/Å)
H
90°
I

Fig. S1. Structure of a monomeric Hrd1-Hrd3 complex.
(**A**) The Hrd1-Hrd3 complex was purified in different detergents and subjected to size-exclusion chromatography. The left panel shows the elution profiles, and the right panel the analysis of fractions by SDS-PAGE and Coomassie-blue staining. Note that Hrd3 dissociates from the complex in DM or DDM, but not in DMNG or LMNG. (**B**) Negative-stain EM of Hrd1-Hrd3 complexes purified in different detergents. Each Hrd3 molecule is visualized as two blobs. Note that there are two Hrd3 molecules associated with each micelle in DM, and only one in DMNG or LMNG. (**C**) Purified CPY* was labeled with the dye Alexa800 and incubated for different time periods with ATP, ubiquitin, ubiquitin-activating and -conjugating enzymes, and Hrd1-Hrd3 complex, purified in DM or DMNG/digitonin. A control was performed without ATP. All samples were analyzed by SDS-PAGE and fluorescence scanning. Note that the complex has lower activity in DM than DMNG. (**D**) Monomeric Hrd1-Hrd3 complex was purified with a streptavidin resin and subjected to size-exclusion chromatography. The right panel shows a Coomassie-stained gel of the purified complex. (**E**) Representative cryo-EM image with selected particles highlighted by green circles. The right panel shows representative 2D class averages of picked particles. (**F**) Image processing workflow for 3D classification and refinement. Shown are views of 3D reconstructions parallel to the membrane, with percentages of the particles in each class indicated. The class shown in pink was used for further analysis. The mask indicated was used for focused refinement. **(G)** Fourier shell correlation (FSC) curves, with indicated resolution at FSC = 0.143. Some FSC calculations were performed with the indicated mask. (**H**) Two different views of the final density map coloured according to local resolution. (**I**) Euler angle distribution in two different views.

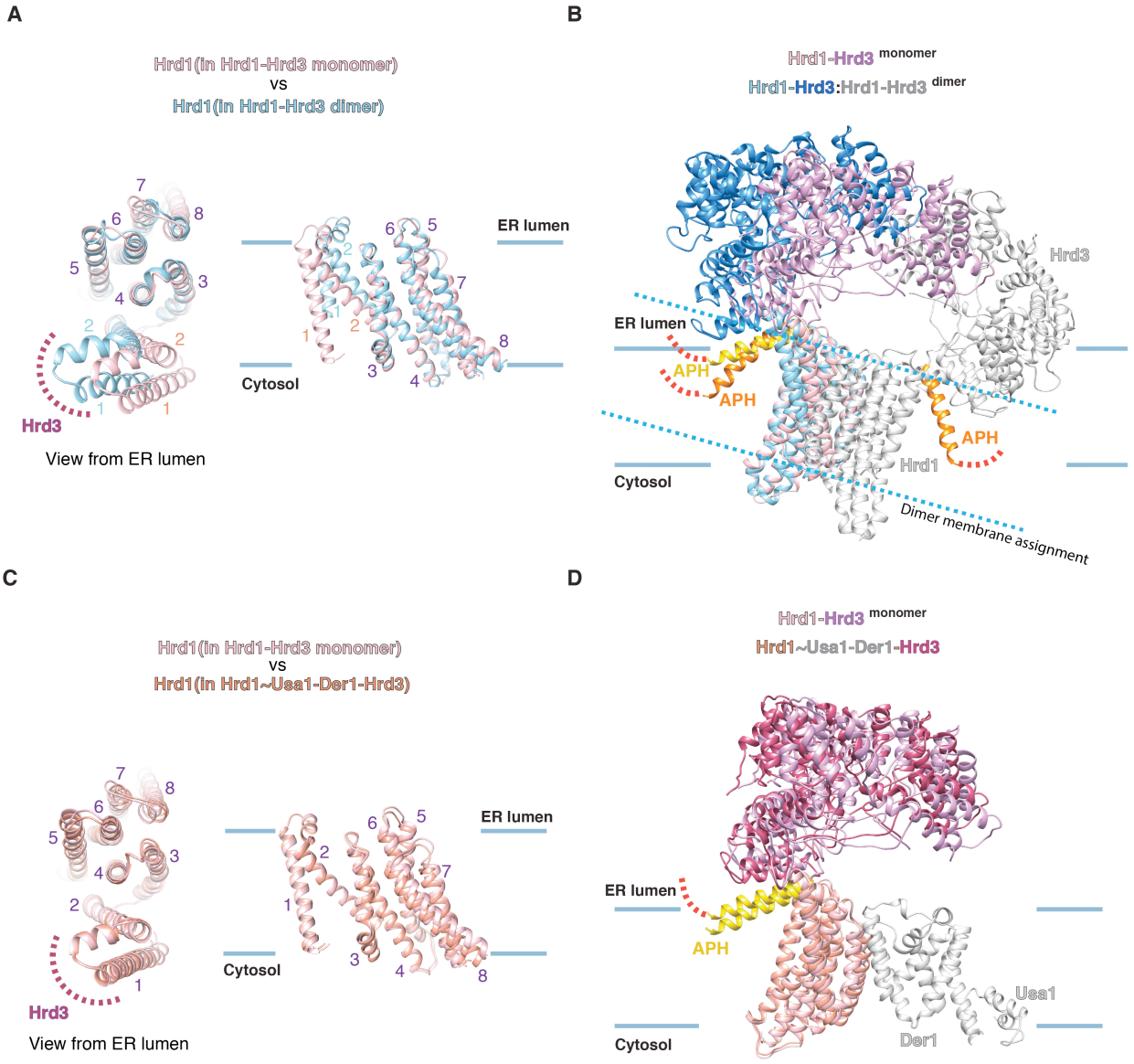

Fig. S2. Hrd1 in the Hrd1-Hrd3 monomer, Hrd1-Hrd3 dimer, and Hrd1~Usa1-Der1-Hrd3 complex.

(**A**) Hrd1 in the monomeric Hrd1-Hrd3 complex (pink) was aligned with Hrd1 from the previous Hrd1-Hrd3 dimer structure (light blue) (*25*). Hrd3 was omitted for clarity. Hrd1 is shown in cartoon representation in views from the ER lumen and the side. The numbers refer to the TMs of Hrd1. The dotted curve indicates that Hrd3 binds to the loop between TM1 and 2. (**B**) Side view as in (A), but with Hrd3 added. The second copies of Hrd1 and Hrd3 in the dimer are shown in grey. An amphipathic helix (APH) of Hrd3 is highlighted in yellow and orange in the monomer and dimer, respectively. No density was visible in the maps for the hydrophilic segment following the APH (shown as a dotted line). The solid and broken blue lines indicate the assigned membrane boundaries in the monomer and dimer structures, respectively. (**C**) As in (A), but comparing Hrd1 in the monomeric Hrd1-Hrd3 complex (pink) and the Hrd-Usa1-Der1-Hrd3 complex (salmon). (**D**) As in (C), but with Hrd3 and Der1-Usa1 added.

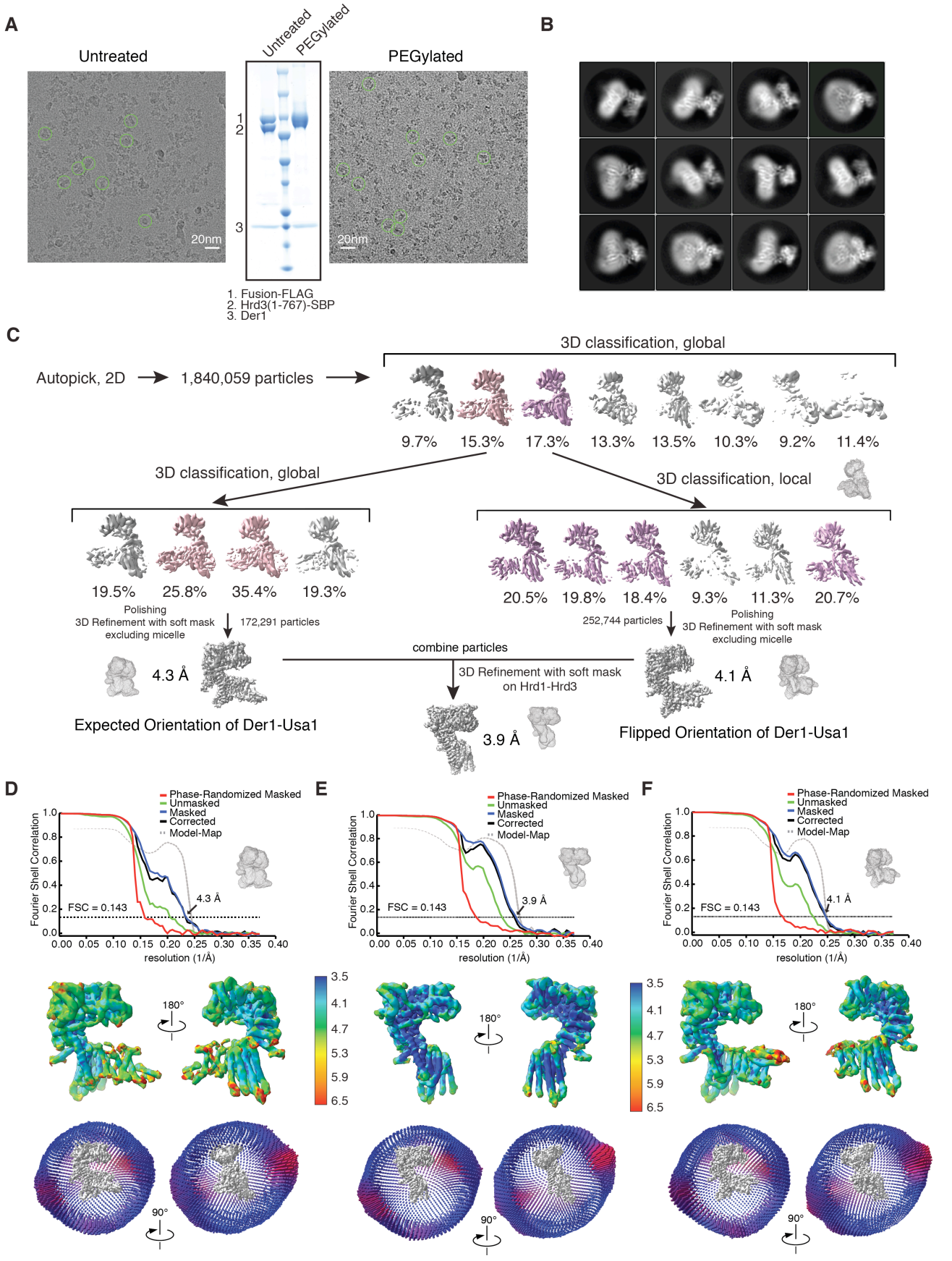
A
Untreated
PEGylated
Untreated
PEGylated
20nm
20nm
1
2
3
1. Fusion-FLAG
2. Hrd3(1-767)-SBP
3. Der1
B
C
Autopick, 2D
1,840,059 particles
3D classification, global
9.7%
15.3%
17.3%
13.3%
13.5%
10.3%
9.2%
11.4%
3D classification, global
3D classification, local
19.5%
25.8%
35.4%
19.3%
Polishing
3D Refinement with soft mask
excluding micelle
172,291 particles
20.5%
19.8%
18.4%
9.3%
11.3%
20.7%
252,744 particles
Polishing
3D Refinement with soft mask
excluding micelle
combine particles
3D Refinement with soft mask
on Hrd1-Hrd3
4.3 Å
4.1 Å
3.9 Å
Expected Orientation of Der1-Usa1
Flipped Orientation of Der1-Usa1
D
E
F
Phase-Randomized Masked
Unmasked
Masked
Corrected
Model-Map
Fourier Shell Correlation
resolution (1/Å)
FSC = 0.143
4.3 Å
3.9 Å
4.1 Å
180°
90°
3.5
4.1
4.7
5.3
5.9
6.5

Fig. S3. Cryo-EM analysis of the Hrd1~Usa1-Der1-Hrd3 sub-complex.
(**A**) The left and right images show representative cryo-EM images of the complex. The sample remained untreated or was treated with low-molecular PEG (PEGylated) before applying it to EM grids. The central panel shows an SDS-gel of the two samples after staining with Coomassie blue. The bands are numbered and correspond to the indicated proteins. (**B**) Representative 2D class averages of picked particles. (**C**) Image processing workflow for 3D classification and refinement. Shown are views of 3D reconstructions parallel to the membrane, with percentages of the particles in each class indicated. The classes shown in pink were used in the further analysis. Masks used are indicated. (**D**) Fourier shell correlation (FSC) curves for the particle class with the expected orientation of Der1-Usa1, with indicated resolution at FSC = 0.143. Some FSC calculations were performed with the indicated mask. The panel below shows two different views of the final map coloured according to local resolution. The lowest panel shows the Euler angle distribution in two different views. (**E**) As in (D), but for the particle class locally refined using a mask surrounding Hrd1-Hrd3. (**F**) As in (D), but for the particle class with flipped orientation of Der1-Usa1.

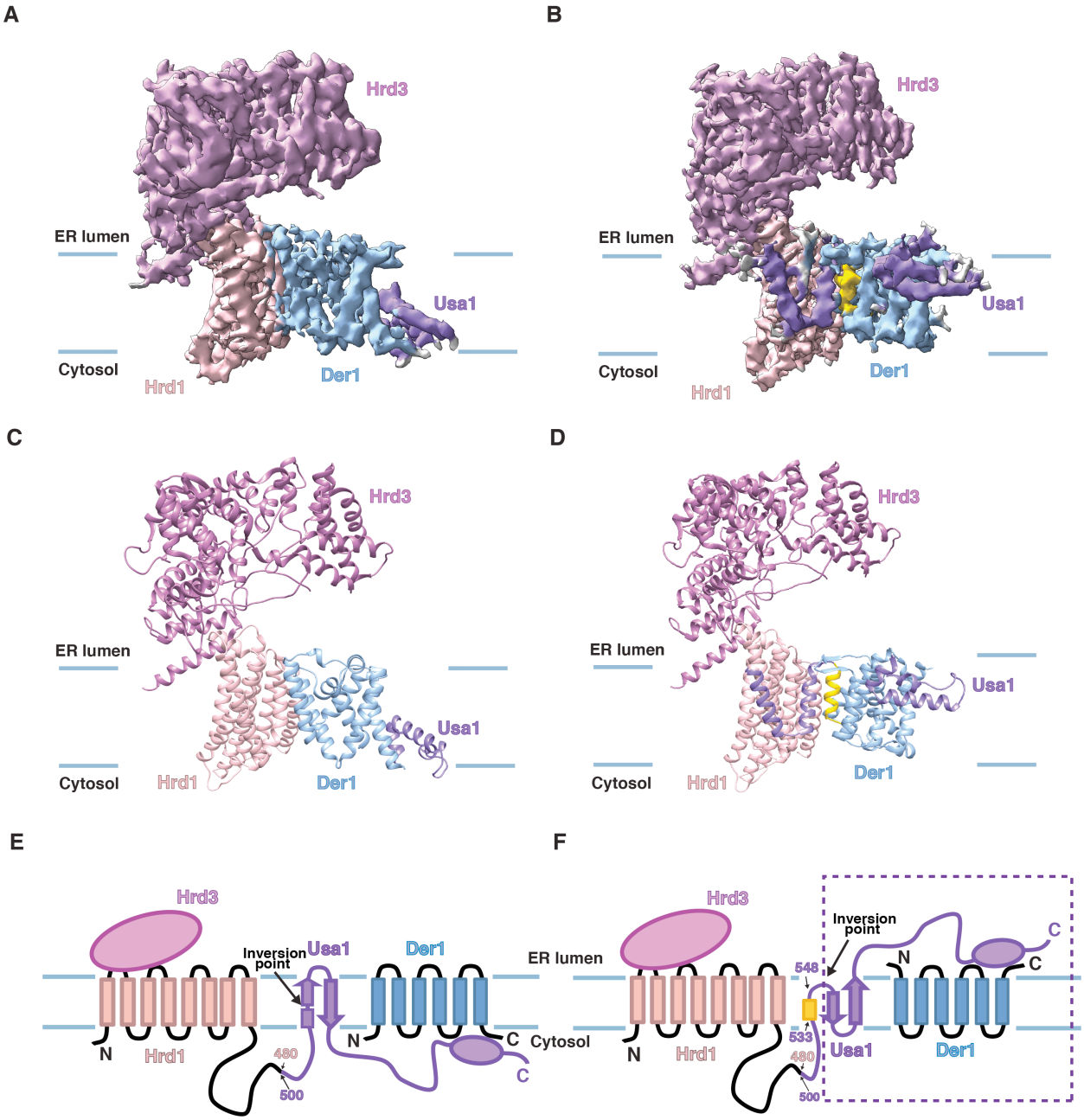

Fig. S4. Cryo-EM maps and models for the Hrd1~Usa1-Der1-Hrd3 sub-complex.
(**A**) Cryo-EM map of a particle class in which Der1-Usa1 have the expected orientation relative to Hrd1-Hrd3. The membrane boundaries are indicated by blue lines. (**B**) As in (A), but for a particle class in which Der1-Usa1 have a flipped orientation relative to Hrd1-Hrd3. The segment in yellow belongs to Usa1. (**C**) Models for the Hrd1 complex components in cartoon representation, based on the map shown in (A). (**D**) As in (C), but based on the map shown in (B). (**E**) Scheme of the topologies of the Hrd1 complex components. (**F**) Topologies in the structure with flipped Der1-Usa1 orientation. Hrd1 and Hrd3 maintain their topology. The C-terminal region of Hrd1 fused to the N-terminal region of Usa1 also remains in the cytosol, as in the correct orientation. The Usa1 segment shown in yellow spans the membrane. All residues following an inversion point in the following loop are on the wrong side of the membrane (dotted box), resulting in a flipped orientation of Der1-Usa1.

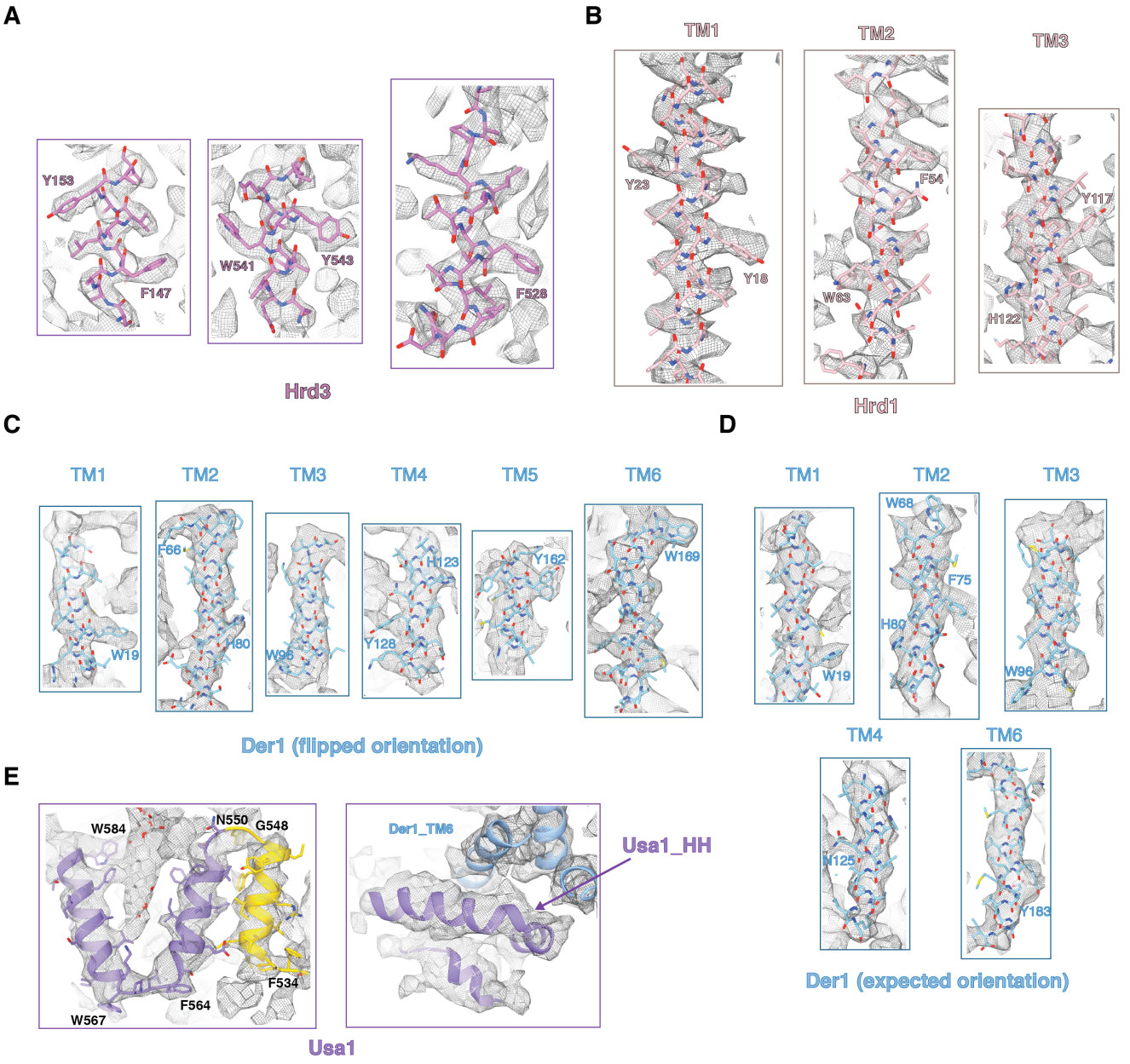

Fig. S5. Examples of the fit of the models into the maps of the Hrd1~Usa1-Der1-Hrd3 complex. **(A)** Map and model for selected segments of Hrd3. (**B**) As in (A), but for the indicated TMs of Hrd1. (**C**) As in (A), but for the indicated segments of Der1 in the structure with flipped Usa1/Der1 topology. (**D**) As in (A), but for the indicated segments of Der1 in the structure with the expected Usa1/Der1 topology. (**E**) As in (A), but for Usa1 in the structure with flipped Usa1/Der1 topology. The left panel shows the two TMs in purple and the additional membrane-spanning segment in yellow. The right panel shows the C-terminal domain, with the hydrophobic helix (HH) interacting with TM6 of Der1.

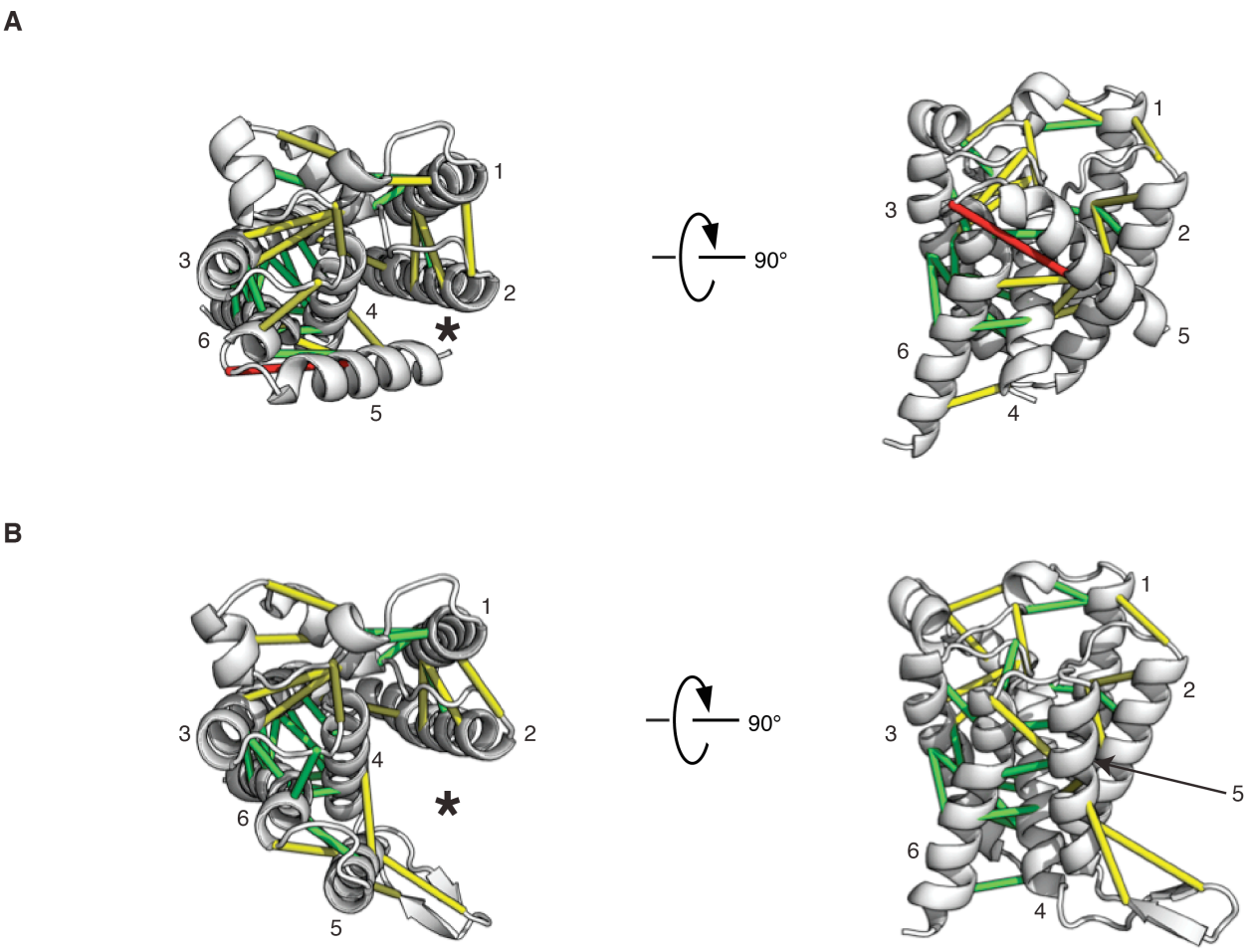

Fig. S6. Evolutionary coupling of Der1 residues.
(**A**) Predicted contacts between amino acid residues of Der1. Evolutionary coupling of Der1 residues from different fungal species were used to predict statistically most likely contacts between residue pairs. These were mapped onto the structure of Der1 derived from the EM map containing Der1-Usa1 in the correct orientation. Shown are views from ER lumen and the side, with contacts < 5Å in green, 5-10Å in yellow, and > 10Å in red. Only contacts with sequence separation >6 and P(contact) >0.95 are shown. (**B**) As in (A), but for the Der1 structure derived from the map with flipped Der1-Usa1 orientation. Note that there are no couplings between TM2 and TM5, consistent with their variable distance during lateral gate opening.

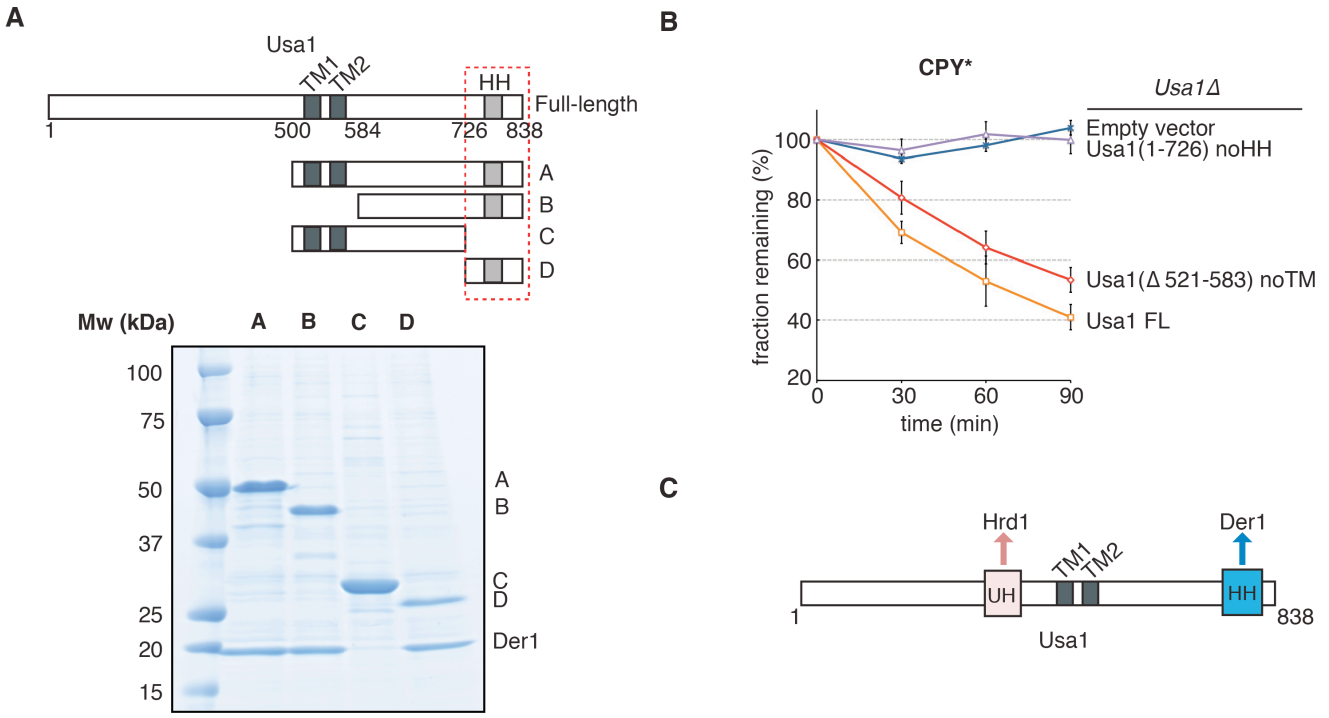

Fig. S7. Usa1 interacts with Der1 through a C-terminal, functionally essential domain.
(**A**) The indicated deletion constructs of Usa1 (A-D) were C-terminally tagged with SBP and co-expressed in *S. cerevisiae* with untagged Der1. The samples were bound to streptavidin beads, eluted, and subjected to gel filtration. The peak fractions were analyzed by SDS-PAGE and Coomassie-blue staining. The C-terminal domain of Usa1 (indicated in the scheme by a dotted red box), including a hydrophobic helix (HH), is necessary for interaction with Der1. (**B**) The degradation of CPY* was tested in cycloheximide-chase experiments using cells lacking endogenous Usa1 and expressing the indicated Usa1 constructs from low-copy CEN plasmids (FL, full-length). Shown are means and standard deviations of three independent experiments. (**C**) Usa1 interacts through its UH domain with Hrd1 and through its C-terminal domain with Der1.

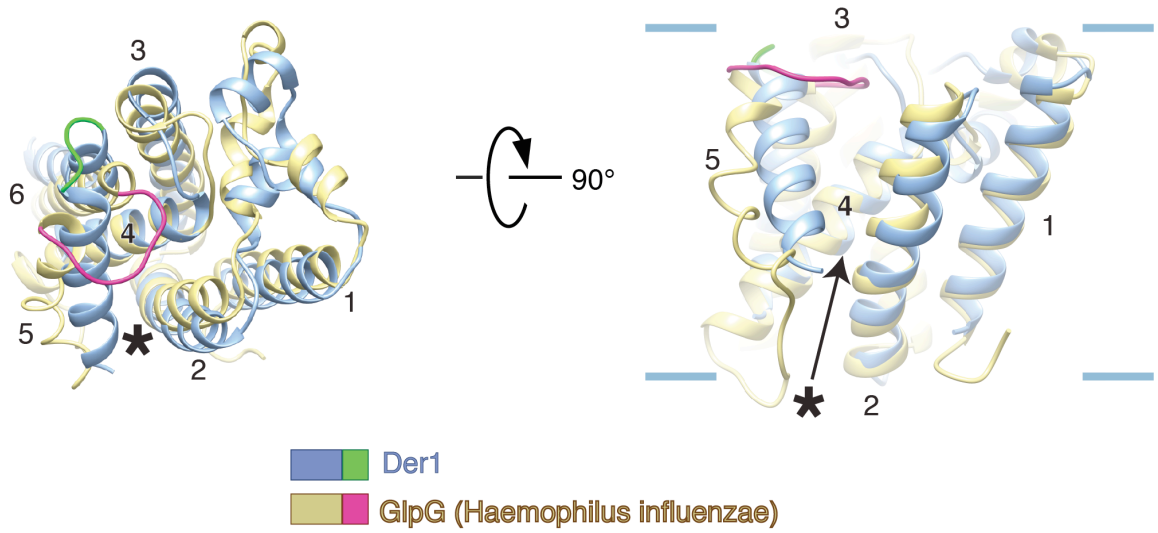

Fig. S8. Comparison of the structures of Der1 and the rhomboid protease glpG from *Haemophilus influenzae*.
The structure of Der1 was aligned with that of *H. influenzae* glpG (PDB code 2NR9). The proteins are shown in cartoon representation. Shown are views from the lumen and the side. The stars indicate the location of the lateral gate. Both proteins have similarly closed lateral gates. The TM5-TM6 loops of Der1 and glpG are highlighted in green and red, respectively.

A

```
                    Cytosol          TM1
Derlin-1_hs --MSDIGDWFRSIPAITRYWFAATVAVPLVGKLGLISPAYLFLWPEAFLYRFQIWRPITA 58
Derlin-1_ce ---MDLENFLLGIPIVTRYWFLASTIIPLLGRFGFINVQWMFLQWDLVVNKFQFWRPLTA 57
Derlin-2_hs MAYQSLRLEYLQIPPVSRAYTTACVLTTAAVQLELITPFQLYFNPELIFKHFQIWRLITN 60
Derlin-3_mm MAGQRLAAGFLQVPAVTRAYTAACVLTTAAVQLELLSPFQLYFNPHLVFRKFQVWRLITT 60
Derlin-3_hs MAWQGLAAEFLQVPAVTRAYTAACVLTTAAVQLELLSPFQLYFNPHLVFRKFQVWRLVTN 60
Der1_sc     -MDAVILNLLGDIPLVTRLWTIGCLVLSGLTSLRIVDPGKVVYSYDLVFKKGQYGRLLYS 59

                         TM2          Cytosol          TM3
Derlin-1_hs TFYFPVGPGTGFLYLVNLYFLYQYSTRLETGAFDGRPADYLFMLLFNWICIVITGLAMDM 118
Derlin-1_ce LIYYPVTPQTGFHWLMMCYFLYNYSKALESETYRGRSADYLFMLIFNWFFCSGLCMALDI 117
Derlin-2_hs FLFFGP---VGFNFLFNMIFLYRYCRMLEEGSFRGRTADFVFMFLFGGFLMTLFGLFVSL 117
Derlin-3_mm FLFFGP---LGFGFFFNMLFVFRYCRMLEEGSFRGRKADFVFMFLFGGVLMTLLGFLGSL 117
Derlin-3_hs FLFFGP---LGFSFFFNMLFVFRYCRMLEEGSFRGRTADFVFMFLFGGVLMTLLGLLGSL 117
Der1_sc     IFDYGA---FNWISMINIFVSANHLSTLEN-SFNLRRKFCWIIFLLLVILVKMTSIEQPA 115

                    TM4          Cytosol          TM5      TM6
Derlin-1_hs QLLMIPLIMSVLYVWAQLN-RDMIVSFWFGTRFKACYLPWVILGFNYIIGGSVINELIG- 176
Derlin-1_ce YFLLEPMVISVLYVWCQVN-KDTIVSFWFGMRFPARYLPWVLWGFNAVLRGGGTNELVG- 175
Derlin-2_hs VFLGQAFTIMLVYVWSRRN-PYVRMNFFGLLNFQAPFLPWVLMGFSLLLGNSIIVDLLG- 175
Derlin-3_mm FFLGQALMAMLVYVWSRRS-PHVRVNFFGLLNFQAPFLPWALMGFSLLLGNSVVTDLLG- 175
Derlin-3_hs FFLGQALMAMLVYVWSRRS-PRVRVNFFGLLTFQAPFLPWALMGFSLLLGNSILVDLLG- 175
Der1_sc     ASLGVLLHENLVYYELKKNGNQMNVRFFGAIDVSPSIFPIYMNAVMYFVYKRSWLEIAMN 175

                    TM6                          Cytosol
Derlin-1_hs NLVGHLYFFLMFRYPMDLGGRNFLSTPQFLYRWLPSRRGGVSGFGVPPASMRRAADQNGG 236
Derlin-1_ce ILVGHAYFFVALKYPDEYG-VDLISTPEFLHRLIPDEDGGIHGQ----DGNIRGARQQPR 230
Derlin-2_hs IAVGHIYFFLEDVFPNQPGGIRILKTPSILKAIFDTPDEDPNYN--------PLPEERPG 227
Derlin-3_mm ILVGHIYYFLEDVFPNQPGGKRLLLTPSVLKLLLDDPQEDPDYL--------PLPEEQP- 226
Derlin-3_hs IAVGHIYYFLEDVFPNQPGGKRLLQTPGFLGLQSSKAPAGSSLT--------IWTQQSQG 227
Der1_sc     FMPGHVIYYMDDIIGKIYG-IDLCKSPYDWFRNTETP---------------------- 211
```

B

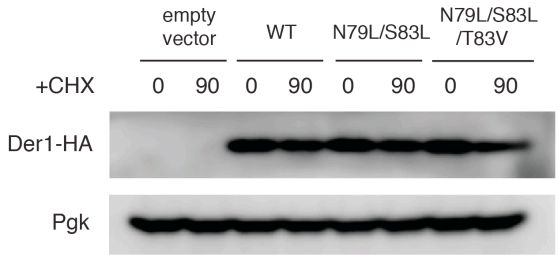

Fig. S9. Sequence alignment of Der1-related proteins and stability of Der1 mutants.
(**A**) Amino acid sequence alignment of *S. cerevisiae* (s.c.) Der1 with the Der1-related Derlins from *H. sapiens* (h.s.), *C. elegans* (c.e.), and *M. musculus* (m.m.). The positions of the TM segments and cytosolic loops, as derived from the structure of Der1, are indicated. Note that the luminal loop between TMs 5 and 6 is short in all species. Residues highlighted in yellow form a hydrophilic surface on the cytosolic side of TM2. They were mutated in S.c. Der1 in **Fig. 4G**. A conserved Pro residue in TM5 is highlighted. (**B**) A cycloheximide (CHX)-chase experiment as in **Fig. 4G** was performed, except that the cells expressed Der1-HA or the indicated tagged Der1 mutants. The samples were subjected to SDS-PAGE. Immunoblotting was performed with HA antibodies to test for the stability of Der1-HA, and with phosphoglycerate kinase (Pgk) antibodies to control for equal sample loading.

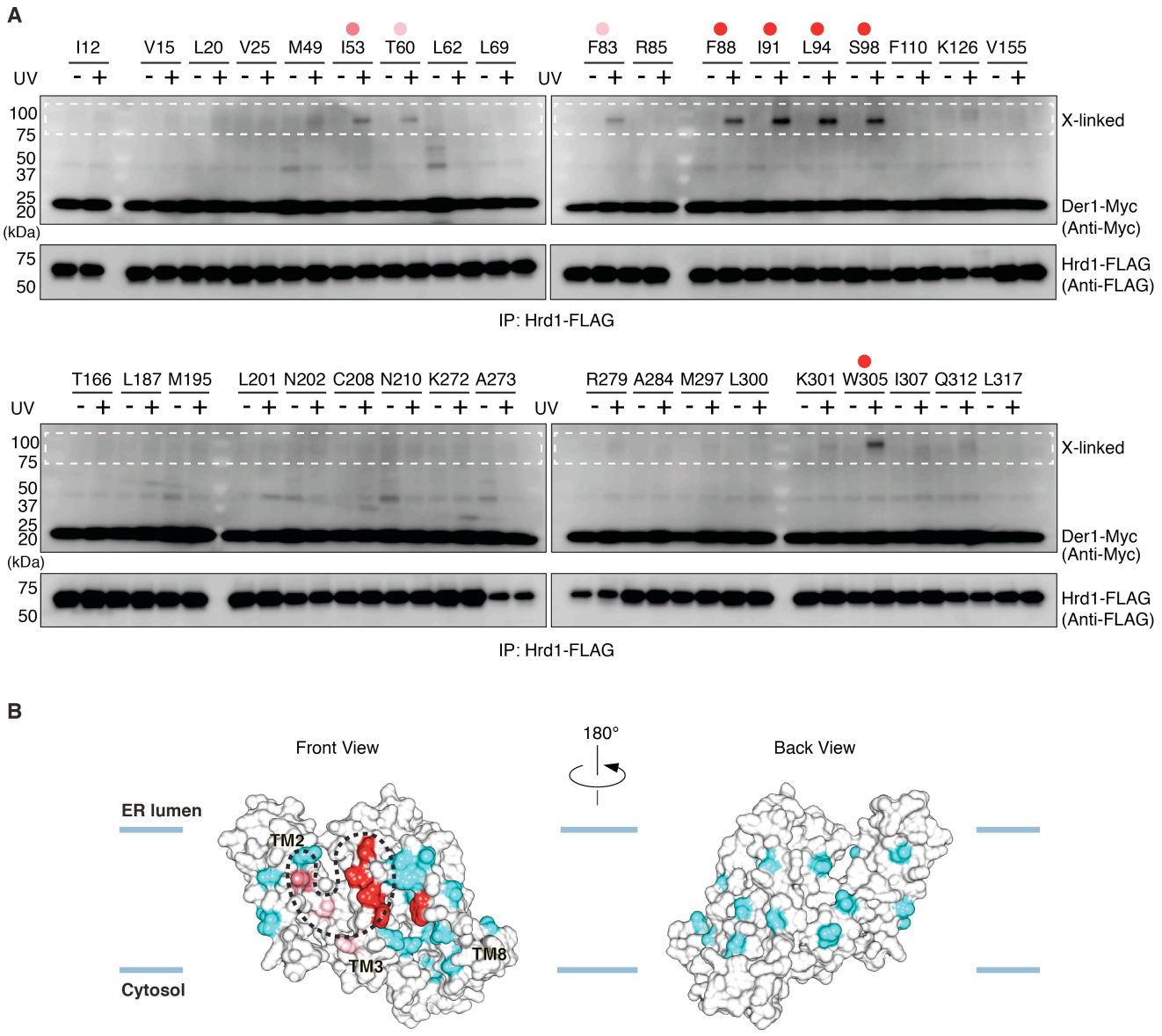

Fig. S10. Probing the proximity of Hrd1 and Der1 by photo-crosslinking.
(**A**) Photo-reactive benzophenone probes were incorporated at different positions into FLAG-tagged Hrd1 by suppression of amber codons. Suppression was achieved in *S. cerevisiae* cells by expression of a modified tRNA-synthetase that charges a suppressor tRNA with the photoreactive amino acid analog benzoyl phenylalanine. The cells also expressed Myc-tagged Der1. After UV irradiation, as indicated, cell lysates were subjected to immunoprecipitation with FLAG-antibodies, followed by SDS-PAGE and immunoblotting with FLAG- and Myc- antibodies. Crosslinked products appear in the indicated region of the gel (white, broken box). The intensities of Hrd1-Der1 crosslinks are qualitatively indicated by dots colored in different shades of red. (**B**) Positions that gave crosslinks to Der1 are mapped in shades of red onto a space-filling model of Hrd1. In the left panel, the Hrd1 funnel is in the front. The boundary of the footprint of Der1 on Hrd1 is indicated by a broken line. In the right panel, the Hrd1 funnel is in the back. Positions that did not crosslink are shown in cyan.

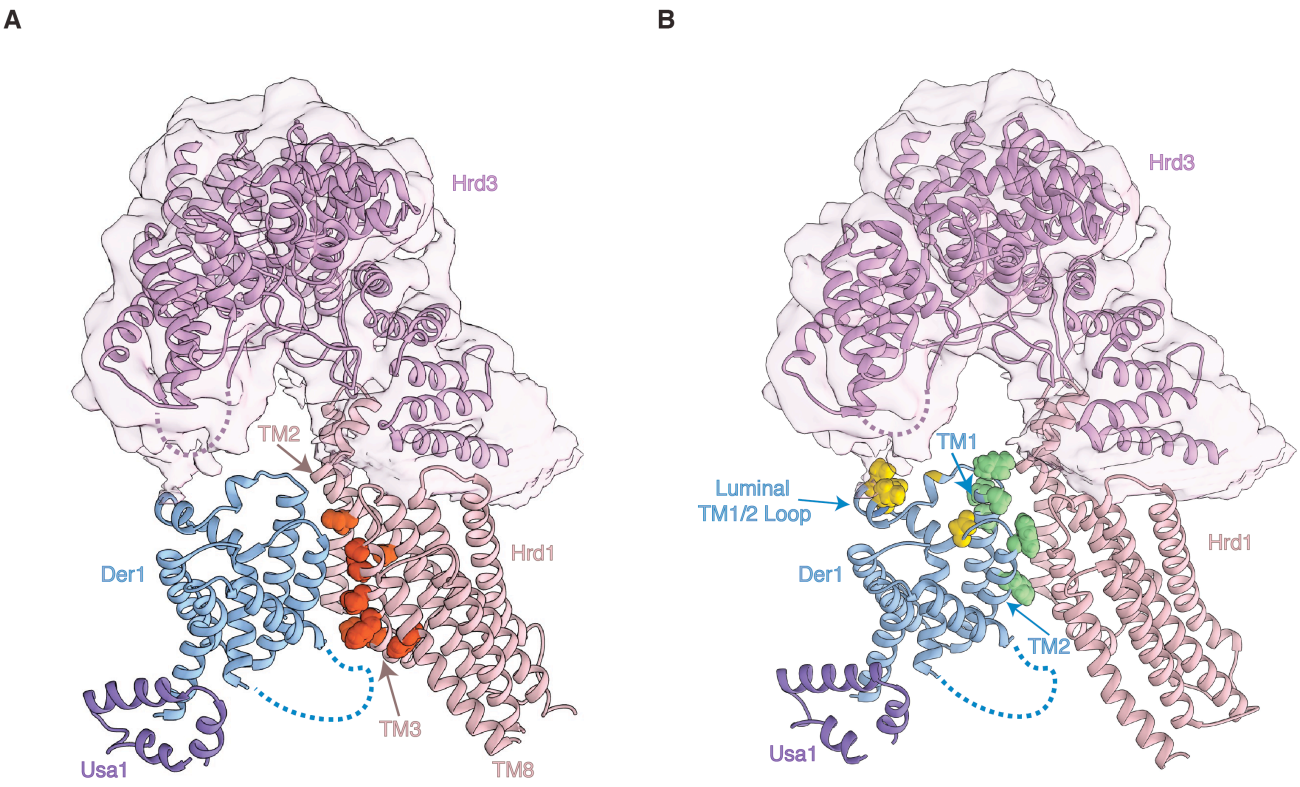

Fig. S11. Amino acid residues at the interface of Hrd1 and Der1.
(**A**) Residues in Hrd1 that crosslink to Der1, as determined from photo-crosslinking experiments with probes in Hrd1 (**Fig. S10**), are shown in red. One residue in TM8 of Hrd1 probably crosslinks to the cytosolic TM 4/5 loop of Der1, which is invisible in the cryo-EM map and shown as a broken line. (**B**) Residues in Der1 that crosslink to Hrd1, as determined by previous photo-crosslinking experiments (*22*), are shown in green. Der1 residues in the TM1/2 loop crosslinking to Hrd3 are shown in yellow.

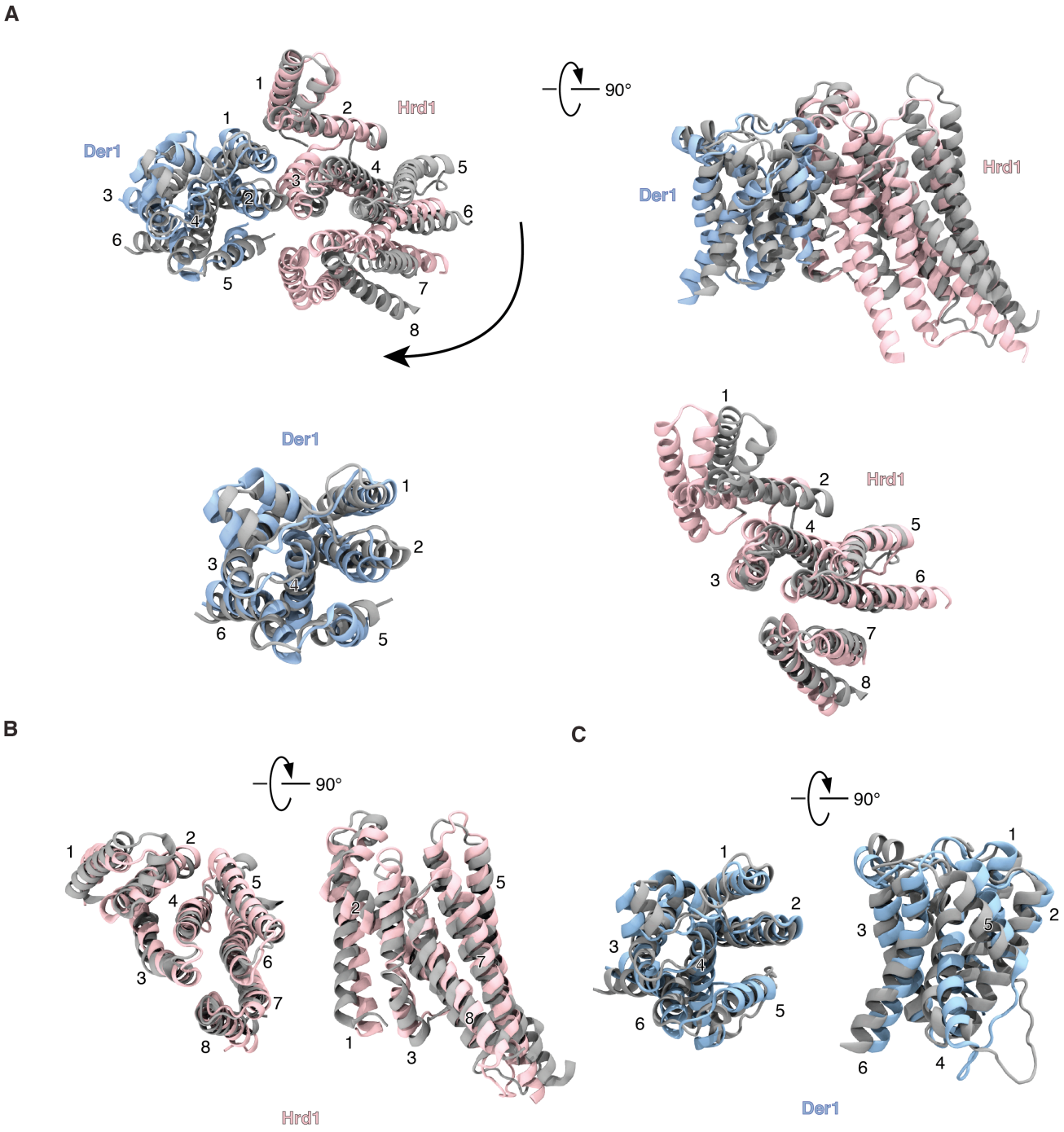

Fig. S12. Stability of structures during MD simulations.
(**A**) All-atom MD simulation of the unrestrained Hrd1-Der1 complex in a membrane consisting of a 1:1 mixture of POPC and DOPC. Der1 lacked the TM4/5 loop that is invisible in the cryo-EM map. Shown is the superposition of the Hrd1-Der1 structures before (grey) and after (pink and blue) MD simulation for 1.2 ms in views from the lumen and the side. The alignment is based on TMs 1 and 2 of Hrd1. The arrow indicates a movement of Hrd1's TM 3-8 relative to TMs 1/2. Water, ions, and lipids are not shown for clarity. The lower left panel shows a comparison of the structures with the alignment based on Der1. A view from the lumen is shown, with Hrd1 omitted for clarity. The lower right panel shows the comparison with alignment based on TM 3-8 of Hrd1. A view from the lumen is shown,

with Der1 omitted for clarity. (**B**) All-atom MD simulation of Hrd1 alone. Shown is the superposition of the Hrd1 structures before (grey) and after (pink) MD simulation for 1 ms in views from the lumen and the side. (**C**) As in (B), but for Der1. The structures before and after the simulation are shown in grey and blue, respectively.

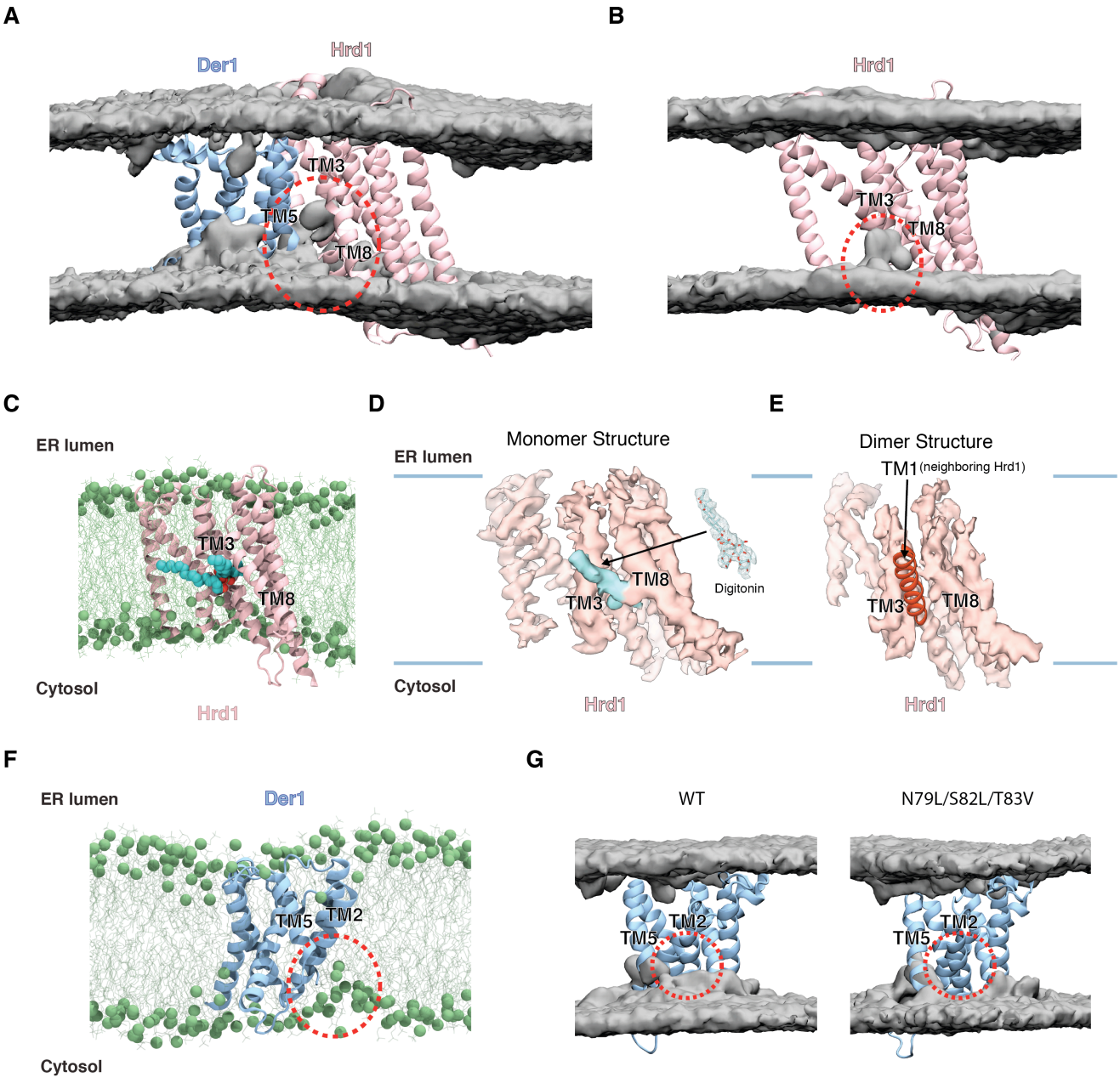

Fig. S13. Position of lipid molecules around Hrd1 and Der1.
(**A**) All-atom unrestrained MD simulation of the Hrd1-Der1 complex in a membrane consisting of a 1:1 mixture of POPC and DOPC. Der1 lacked the TM4/5 loop that is invisible in the cryo-EM map. Shown are the Hrd1 and Der1 models in cartoon representation and the average head group phosphate density (grey). The oval indicates head groups penetrating into the membrane on the cytosolic side of the lateral gate between TMs 3 and 8. The penetration seen on the left of Der1 is artificially caused by the omission of the C-terminal domain of Usa1 in the simulations. (**B**) As in (A), but for MD simulation of Hrd1 alone (1 ms). (**C**) As in (B), but a snap-shot of the Hrd1 simulation. Phosphorus atoms in lipid head groups are shown as green spheres and lipid tails as green lines. A phospholipid molecule in the cytosolic funnel of Hrd1 is shown with the head group in red and the hydrocarbon chains in cyan calottes. (**D**) Cryo-EM map (salmon) of Hrd1 after focused refinement of the Hrd1-

Hrd3 region of the Hrd1~Usa1-Der1-Hrd3 complex. The density in cyan is at a similar position as in (C) and could be modeled with a digitonin molecule (shown on the right). (**E**) As in (D), but for the previous dimeric Hrd1-Hrd3 complex (*25*). In this case, TM1 of the neighboring Hrd1 molecule (red helix in cartoon) blocks the binding site of the detergent molecule. (**F**) As in (C), but for Der1 (1 ms simulation). (**G**) As in (F), but showing the average head group phosphate density (grey) for MD simulations of wild-type (WT) Der1 and for a Der1 variant in which three hydrophilic residues on the cytosolic side of TM2 were mutated to hydrophobic residues (**Fig. 4G**). Note that head groups penetrate into the membrane on the cytosolic side of the lateral gate between TMs 2 and 5 in the wild-type, but not the mutant (red oval).

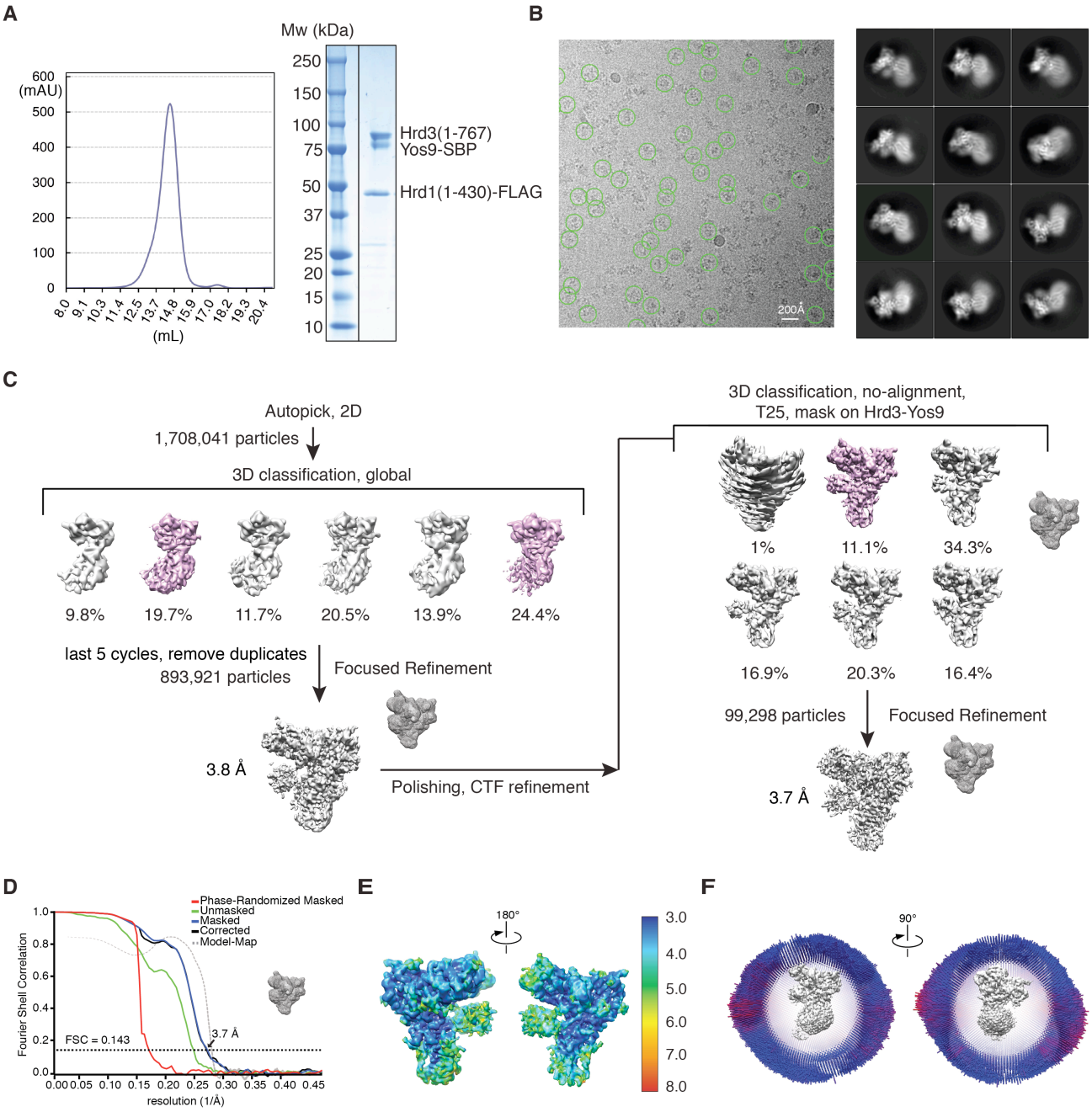

Fig. S14. Cryo-EM analysis of the Hrd1-Hrd3-Yos9 sub-complex.
(**A**) FLAG-tagged Hrd1 was expressed together with SBP-tagged Yos9 and untagged luminal domain of Hrd3 in *S. cerevisiae* cells. The complex was purified with streptavidin- and anti-FLAG resins, followed by size-exclusion chromatography. Shown is the elution profile in gel filtration. The pooled material was subjected to SDS-PAGE and Coomassie-blue staining (right panel) and used for cryo-EM analysis. (**B**) Representative cryo-EM image with selected particles marked by green circles. The right panel shows representative 2D class averages of picked particles. (**C**) Image processing workflow for 3D classification and refinement. Shown are views of 3D reconstructions parallel to the membrane, with percentages of the particles in each class. The classes selected for further analysis are shown in pink. Masks used for classification and refinement are indicated. **(D)** Fourier shell correlation (FSC) curves with indicated resolution at FSC = 0.143. Some FSC calculations used the mask shown on the

side. (**E**) Two different views of the final density map colored according to local resolution. (**F**) Euler angle distribution in two different views.

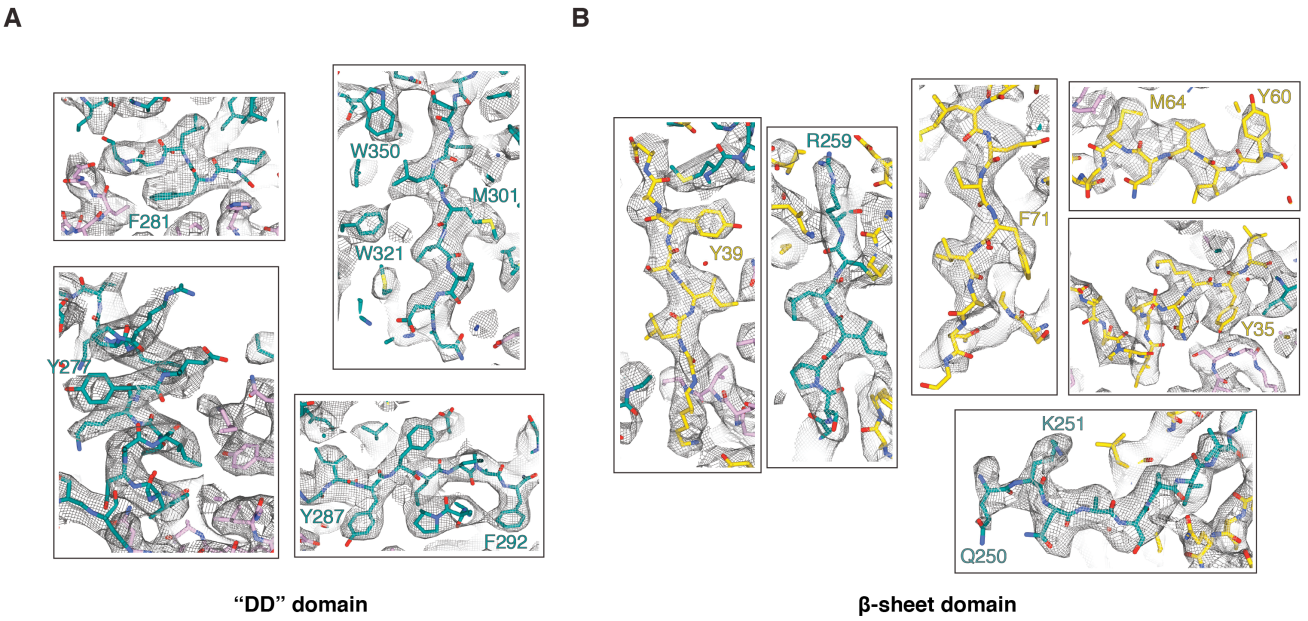
A
F281
W350
M301
W321
Y277
Y287
F292
"DD" domain
B
R259
Y39
F71
M64
Y60
Y35
K251
Q250
β-sheet domain
C
"DD" domain
β-sheet domain
C288
C10
S1
S4
S3
S2
from MRH
to MRH
N
Hrd3
D
"DD" domain
β-sheet domain
MRH domain
Variable
conserved
50°
"DD" domain
MRH domain
β-sheet domain
E
D249
Q250
90°
D249
Q250
MRH domain

Fig. S15. Map and model for Yos9 in the Hrd3-Yos9 complex.
(**A**) Examples of the fit of the model into the map for the "DD" domain of Yos9. (**B**) As in (A), but for the b-sheet domain. (**C**) Model for the b-sheet domain. The strands of the sheet are labeled S1-S4. S4 follows the MRH domain and is intercalated into the middle of the sheet. (**D**) Interaction of Hrd3 with the "DD" and b-sheet domains of Yos9 in two different views. Yos9 domains are shown in cartoon representation and Hrd3 in a space-filling model. The degree of conservation of amino acids in Hrd3 is indicated in different colors (scale on the right). (**E**) Unsharpened map for the MRH domain together with the docked NMR structure (PDB code 6F99; (*47*)). Note that density for amino acids was seen starting from the first residue of the "DD" domain (see map in (B)), which immediately follows the last residue of the MRH domain. All maps are contoured as in Fig. 5.

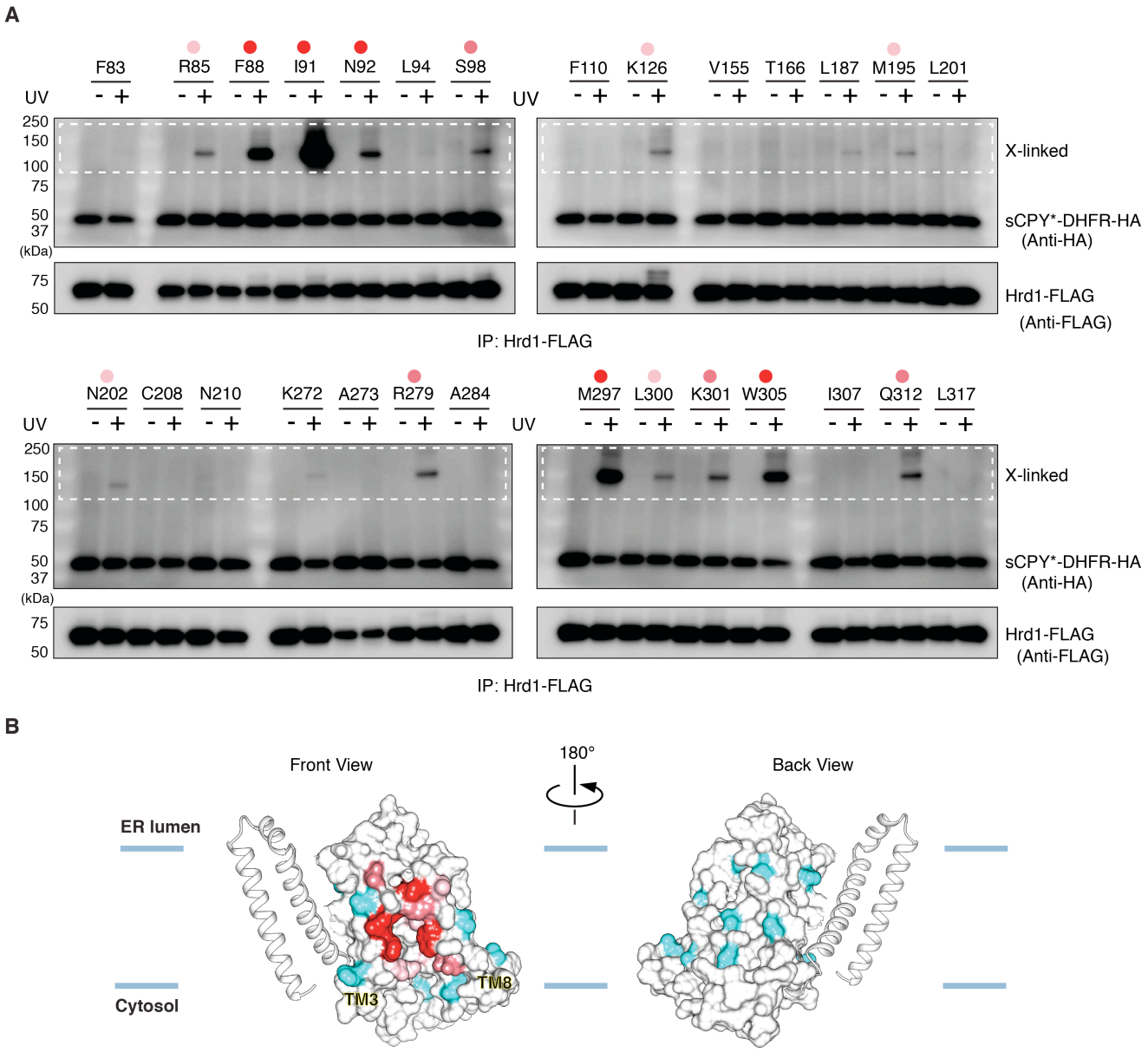

Fig. S16. Probing the proximity of Hrd1 to substrate by photo-crosslinking.
(**A**) Photo-reactive benzophenone probes were incorporated at different positions into FLAG-tagged Hrd1 by suppression of amber codons. The cells also expressed HA-tagged sCPY*-DHFR, an ERAD-L substrate. The cells were UV-irradiated, where indicated, and lysates were subjected to immunoprecipitation with FLAG-antibodies, followed by SDS-PAGE and immunoblotting with FLAG- and HA- antibodies. Crosslinked products appear in the indicated region of the gel (white, broken box). The intensities of Hrd1-Der1 crosslinks are qualitatively indicated by dots colored in different shades of red. (**B**) Positions that gave crosslinks to substrate are mapped in red onto the model of Hrd1. Positions that did not crosslink are shown in cyan. TMs 1 and 3 are shown in cartoon representation and TMs 3-8 as a space-filling model. In the left and right panels, the Hrd1 funnel is in the front and back, respectively.

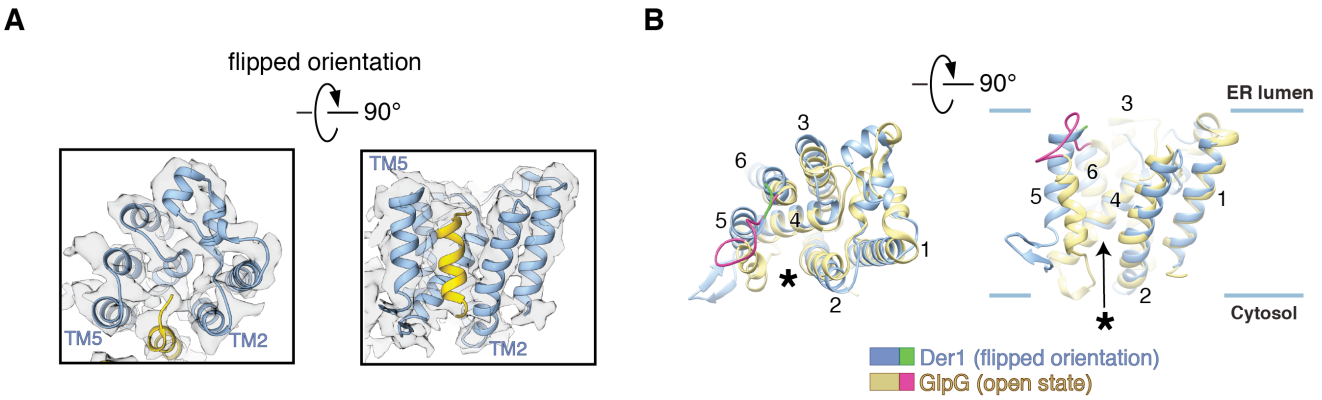

Fig. S17. Der1 in the flipped orientation has an open lateral gate.
(**A**) Shown is the EM map (contoured at 0.028) (grey) for Der1 in the Hrd1~Usa1-Der1-Hrd3 complex with a flipped orientation of Der1-Usa1, together with cartoon models for Der1 (blue) and a membrane-spanning Usa1 helix (yellow). The views are from the lumen and the side. (**B**) Overlay of the structure of Der1 in the flipped orientation (blue) with the open conformation of the *E. coli* rhomboid protein glpG (yellow) (PDB code 2NRF). The membrane-spanning Usa1 segment was omitted for clarity. The TM5-TM6 loops of Der1 and glpG are highlighted in green and red, respectively. The stars indicate the lateral gates. Note that the lateral gate of Der1 in the flipped orientation is wide open.

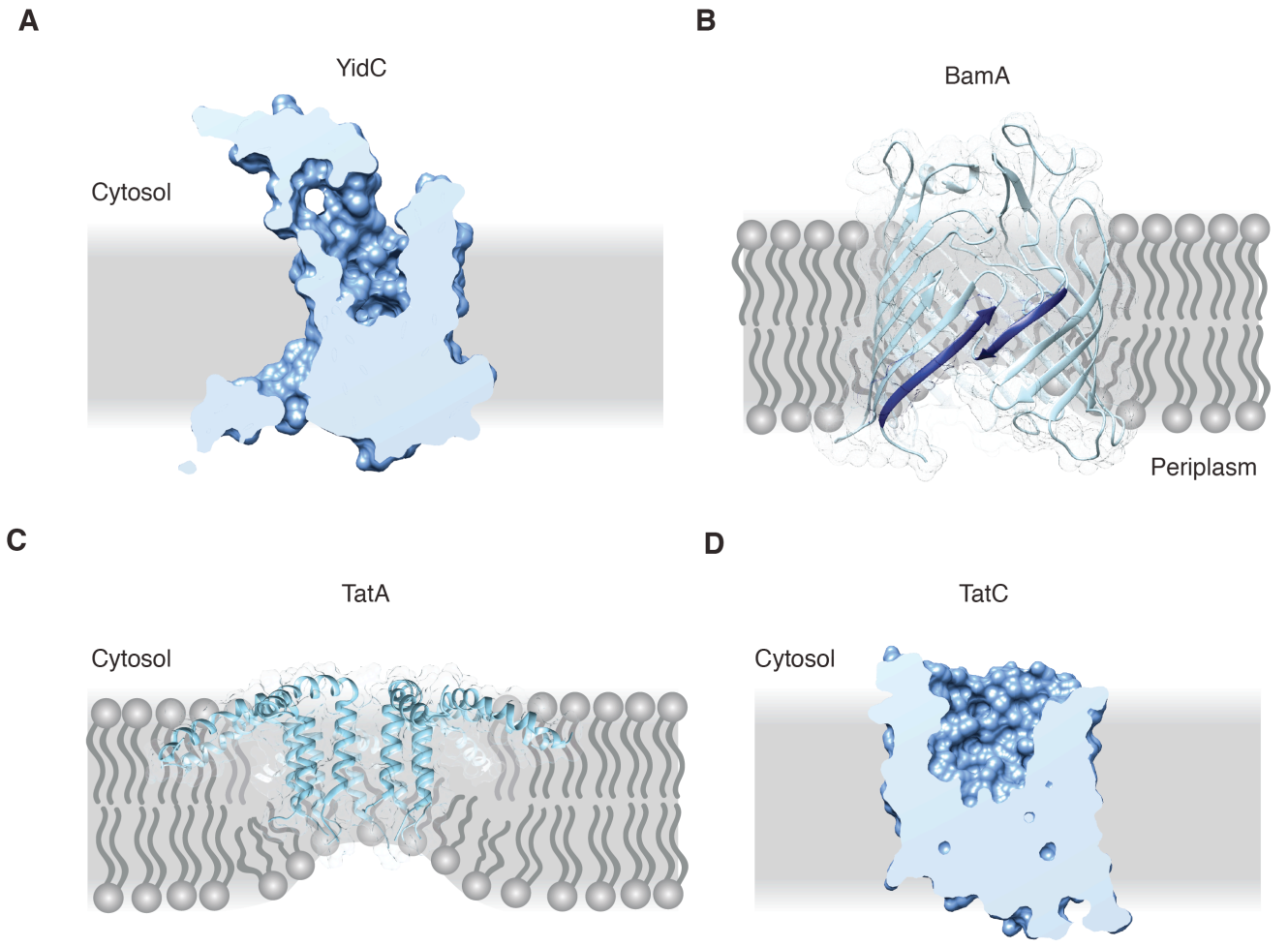

Fig. S18. Translocation proteins inducing a thinned lipid bilayer.
(**A**) Cut through a space-filling model of YidC (PDB code 3WO6). The membrane is indicated in grey. (**B**) Cartoon of the BamA protein (PDB code 4K3B). The b-strands at the lateral gate are highlighted and are located in a region of thinned membrane. Phospholipid molecules are shown schematically. (**C**) Cartoon of the TatA protein with a thinned membrane area induced by the oligomerization of its short TM (PDB code 2LZS). Phospholipid molecules are shown schematically. (**D**) Cut through a space-filling model of TatC (PDB code 4B4A). The membrane is indicated in grey.

Table S1. Statistics for data collection and refinement

Structure	Hrd1-Hrd3 monomer	Hrd1~Usa1-Der1-Hrd3			Hrd3-Yos9
		Hrd1~Usa1-Der1 - Hrd3 (Expected)	Hrd1~Usa1-Der1 - Hrd3 (Flipped)	Hrd1-Hrd3 (focused)	
Data Accession					
PDB	6VJY	6VJZ	6VK0	6VK1	6VK3
EMDB	EMD-21220	EMD-21221	EMD-21222	EMD-21223	EMD-21224
Data Collection					
Microscope	Talos Arctica	Titan Krios			Titan Krios
Voltage (kV)	200	300			300
Exposure navigation	Stage Movement	Stage Movement			Stage Movement &beamshift
Automation software	SerialEM	SerialEM			SerialEM
Detector	Gatan K3 Summit (Counting)	Gatan K2 Summit (Super resolution)			Gatan K3 Summit (Counting)
Energy filter	NA	20 eV			20 eV
Nominal magnification	36k	81k			81k
Pixel Size	1.13 Å	1.35 Å			1.06 Å
Exposure time, frames	3.0 s, 43 frames	10.0 s, 50 frames			3.0 s, 40 frames
Exposure rate ($e^- pixel^{-1} s^{-1}$)	20.3	10.0			16.8
Electron exposure ($e^-/Å^2$)	47.7	54.8			44.9
Defocus range (μm)	-1.5 to -3.2	-1.2 to -3.0			-0.9 to -3.0
Micrographs collected	2385	5890			9706
Reconstruction					
Software	Relion 3.0	Relion 3.0			Relion 3.0
Micrographs used	2303	5457			9180
Particles extracted	878,370	2,057,682			2,650,342
Particles used in refinement	197,173	172,291	252,744	425,035	99,298
Symmetry	C1	C1	C1	C1	C1
Overall resolution (Å) FSC=0.143 (masked)	4.3	4.3	4.1	3.9	3.7
Estimated error/accuracy of translations/rotations	2.83/1.225	2.85/0.91	2.81/0.91	2.82/0.91	1.89/0.83
Map sharpening B-factor ($Å^2$)	-200	-210	-230	-230	-150
Local resolution range (Å)	3.5-6.5	3.5-6.5	3.5-6.5	3.5-5.5	3.0-6.0
Model Refinement					
Software	Phenix	Phenix			Phenix
Model Composition					
Non-hydrogen atoms	7382	9114	9676	7456	7784
Protein residues	883	1093	1160	883	961
B factors ($Å^2$)					
Protein	126.56	114.4	94.09	65.60	57.41
R.M.S. deviations					
Bond length (Å)	0.003	0.006	0.007	0.004	0.006
Bond angle (°)	0.627	0.822	0.818	0.941	0.923
Ramachandran statistics (%)					
Outliers	0.00	0.09	0.00	0.00	0.11
Allowed	4.14	6.15	6.84	4.49	5.09
Favored	95.86	93.76	93.16	95.51	94.80
MolProbity score	1.87	2.24	2.17	1.92	1.95

C-beta deviations	0.00	0.00	0.00	0.00	0.00
CaBLAM outliers (%)	2.22	2.56	2.05	2.69	3.03
All-atom clashscore	11.71	21.41	17.10	12.53	11.98
Poor rotamers (%)	0.1	0.0	0.1	0.0	0.0
model-map CC	0.81	0.79	0.78	0.78	0.8
Model vs. Map FSC					
FSC=0.5 (masked, Å)	4.3	4.3	4.2	4.0	3.7

Table S2. Simulated Systems

Protein	Lipids [No.]	Boxsize [nm]	Total Atoms	Time [µs]
Hrd1 (EM structure)	POPC = 311 DOPC = 311	15 x 15 x 10	233433	1 x 1 µs 2 x 0.5 µs
Der1 (EM structure)	POPC = 196 DOPC = 196	12 x 12 x 10	116976	1 x 1 µs
Der1 (with loop)	POPC = 196 DOPC = 196	12 x 12 x 10	128826	1 x 1 µs
Der1 N79L/S82L/T83V (with loop)	POPC = 196 DOPC = 196	12 x 12 x 10	128991	1 x 1 µs
Hrd1-Der1 (EM structure)	POPC = 297 DOPC = 297	15 x 15 x 10	226320	1 x 1.2 µs